International Journal of Mechanical, Industrial and Aerospace Sciences
ISSN: 2517-9950
Vol:10, No:1, 2016

Increasing Performance of Autopilot Guided Small Unmanned Helicopter

Tugrul Oktay, Mehmet Konar, Mustafa Soylak, Firat Sal, Murat Onay, Orhan Kizilkaya

***Abstract*—**In this paper, autonomous performance of a small manufactured unmanned helicopter is tried to be increased. For this purpose, a small unmanned helicopter is manufactured in Erciyes University, Faculty of Aeronautics and Astronautics. It is called as ZANKA-Heli-I. For performance maximization, autopilot parameters are determined via minimizing a cost function consisting of flight performance parameters such as settling time, rise time, overshoot during trajectory tracking. For this purpose, a stochastic optimization method named as simultaneous perturbation stochastic approximation is benefited. Using this approach, considerable autonomous performance increase (around %23) is obtained.

***Keywords*—**Small helicopters, hierarchical control, stochastic optimization, autonomous performance maximization, autopilots.

I. Introduction

FOR the prior four and five decades Unmanned Air Vehicles (UAVs) have been extensively promoted for military operations as well in commercial applications because of their many advantages with respect to the manned vehicles. Some of these benefits are low cost for manufacturing and operating, flexibility in configuration depending on customer demand and also not risking the pilot's life on hard missions.

UAVs have been applied for electricity companies, fire services and forestry, fisheries, gas and oil supply companies, aerial photography, agriculture, coast guard, conservation, customs and excise, etc. with civilian purposes [1]. They have also been used for military assignments. For instance, they have been used during shadowing enemy fleets, decoying missiles by the emission of artificial signatures, protection of ports from offshore attack for navy, reconnaissance, surveillance of enemy activity, monitoring of nuclear, biological or chemical NBC contamination, location and destruction of land mines for army and long-range, high-altitude surveillance, radar system jamming and destruction, airfield base security, airfield damage assessment for air force. for more UAV applications [1]. In order to achieve mentioned tasks, the rotorcraft-based unmanned aerial vehicles (RUAVs) need to have a confident level of autonomy to withstand its stability following a desired path under embedded guidance, navigation and control algorithm. In [2] a small-scale helicopter was intentioned and applied as a flying test-bed for the drive of developing the autonomous capability. In this study, it was found that the gains of the multi-loop cascaded control architecture can be effectively optimized within the hardware in the loop simulation environment. Several autonomous flight operations are succeeded and it is shown that the prediction from the simulations is in a respectable agreement with the consequence from the flight test. In [3]-[5] different helicopter UAV studies were followed.

T. Oktay is with the Erciyes University, Kayseri, 38039 Turkish Republic (corresponding author phone: +90-533-5186324; e-mail: tugruloktay52@ gmail.com).

M. Konar, M. Soylak, F. Sal and M. Onay are with the Erciyes University, Kayseri, 38039 Turkish Republic.

O. Kizilkaya is with the Teknopark, Kayseri, 38039 Turkish Republic.

II. Helicopter Models

Modeling approach of helicopter models applied herein depends on two main points. First, physics principles and appropriate modeling assumptions are benefited in order to result in nonlinear ordinary differential equations (ODEs). Second, the models capture not only the flight dynamics modes but also blade dynamics modes which are critical for safe and performant operation. In order to get such models multibody dynamics was used to include all important components of a helicopter: fuselage, fully articulated (i.e. both flapping and lead-lagging motions are included) main rotor with 4 blades, empennage, landing gear, tail rotor. The key points for obtaining the helicopter models are given next.

(a) (b)

Fig. 1 Manufactured Helicopter UAV (i.e. ZANKA- Heli-I) (a) Upper View (b) Side View

A. Dynamic and Kinematic Equations of Fuselage

In order to find the nondimensionalized helicopter force and moment Equations (1) and (2) Newton-Euler equations were applied and found that:

$$\begin{aligned}
&\frac{d}{d\psi}\hat{u}+\hat{q}\,\hat{w}-\hat{r}\,\hat{v}+\frac{g\sin(\theta_A)}{\Omega^2\,R}=\frac{X}{\Omega^2\,R\,M_a}\\
&\frac{d}{d\psi}\hat{v}+\hat{r}\,\hat{u}-\hat{p}\,\hat{w}-\frac{g\cos(\theta_A)\sin(\phi_A)}{\Omega^2\,R}=\frac{Y}{\Omega^2\,R\,M_a}\\
&\frac{d}{d\psi}\hat{w}+\hat{p}\,\hat{v}-\hat{q}\,\hat{u}-\frac{g\cos(\theta_A)\cos(\phi_A)}{\Omega^2\,R}=\frac{Z}{\Omega^2\,R\,M_a}
\end{aligned} \tag{1}$$

$$\begin{aligned}
&\frac{d}{d\psi}\hat{p}-\hat{q}\,\hat{r}\left(\frac{I_{yy}}{I_{xx}}-\frac{I_{zz}}{I_{xx}}\right)-\frac{I_{xz}}{I_{xx}}\left(\hat{p}\,\hat{q}+\frac{d}{d\psi}\hat{r}\right)=\frac{L}{I_{xx}\,\Omega^2}\\
&\frac{d}{d\psi}\hat{q}-\hat{p}\,\hat{r}\left(\frac{I_{zz}}{I_{yy}}-\frac{I_{xx}}{I_{yy}}\right)+\frac{I_{xz}}{I_{yy}}\left(\hat{p}^2-\hat{q}^2\right)=\frac{M}{I_{yy}\,\Omega^2}\\
&\frac{d}{d\psi}\hat{r}-\hat{p}\,\hat{q}\left(\frac{I_{xx}}{I_{zz}}-\frac{I_{yy}}{I_{zz}}\right)-\frac{I_{xz}}{I_{zz}}\left(\hat{q}\,\hat{r}-\frac{d}{d\psi}\hat{p}\right)=\frac{N}{I_{zz}\,\Omega^2}
\end{aligned} \tag{2}$$

Moreover, the nondimensionalized kinematic Euler equations are;

$$\begin{aligned}
\hat{p}&=\frac{d}{d\psi}\phi_A-\frac{d}{d\psi}\psi_A\sin(\theta_A)\\
\hat{q}&=\frac{d}{d\psi}\psi_A\cos(\theta_A)\sin(\phi_A)+\frac{d}{d\psi}\theta_A\cos(\phi_A)\\
\hat{r}&=\frac{d}{d\psi}\psi_A\cos(\theta_A)\cos(\phi_A)-\frac{d}{d\psi}\theta_A\sin(\phi_A)
\end{aligned} \tag{3}$$

B. Dynamic and Aerodynamic Forces Acting on Single Blade of Main Rotor

In order to get single blade equations first, integration of infinitesimal aerodynamic and inertial forces and moments acting on blade strips along blade span w.r.t. blade hinge is required and second flapping and lead-lagging spring and damper moments should be included. The infinitesimal aerodynamic force and moment acting on a blade strip in lead-lagging and flapping frame (LLF) are, respectively,

$$d_{LLF}F_{aero}=\frac{\gamma I_b}{2R^3}\begin{bmatrix}0\\ -\left(\theta\,U_T^2-U_P\,U_T\right)\frac{U_P}{U_T}-\frac{1}{a_0}\left(\delta_0+\delta_2\left(\theta-\frac{U_P}{U_T}\right)^2\right)\\ \theta\,U_T^2-U_P\,U_T\end{bmatrix}dx \tag{4}$$

$$d_{LLF}M_{aero}=\begin{bmatrix}0 & -xR\,(d_{LLF}F_{aero})_{III} & xR\,(d_{LLF}F_{aero})_{II}\end{bmatrix}^T \tag{5}$$

U_P and U_T are perpendicular and tangential components of air velocity acting on the blade leading edge, θ is the blade pitch angle, x is the nondimensional location of a generic point on the blade. Via integration over the blade length total blade aerodynamic force and moment are found.

C. Dynamic and Aerodynamic Equations of Multi-Blades

Neglecting higher harmonic terms and using 4 blades for the main rotor, the blade flapping and lead-lagging motions are

$$\Theta_i(\psi)=\Theta_0+\Theta_{1c}\cos(\psi_i)+\Theta_{1s}\sin(\psi_i)+\Theta_{0d}\,(-1)^i \tag{6}$$

where the blade azimuth angle of the blade i is

$$\psi_i=\psi-(\pi/2)(i-1),\ \ i=1,...,4 \tag{7}$$

and Θ is the generic notation for any of the two angles mentioned in the above while Θ_0, Θ_c, Θ_s, and Θ_d are collective, two cyclic and differential components, respectively.

D. Dynamic and Aerodynamic Equations of Multi-Blades

In order to collect helicopter model, all the components outlined above were assembled into the nonlinear equations of the helicopter dynamics. These, derived using Maple, were found in the generic implicit form

$$f(\dot{x},x,\upsilon)=0 \tag{8}$$

where x is the nonlinear state vector comprising the fuselage states (i.e. linear and angular velocities, Euler angles) and blade states (i.e. flapping and lead-lagging states), and υ is the nonlinear control vector comprising two cyclic and a collective control for the main rotor and tail rotor force. For control design, the nonlinear models were linearized around several trim conditions. In Figs. 2-3, flight dynamics modes and flapping modes of ZANKA-Heli-I are given respectively. In Table I, data of ZANKA-Heli-I is summarized. In (12)-(15), state-space models for specific flight conditions are given.

TABLE I
DATA OF ZANKA-HELI-I

Parameters	Units Symbols	Values
Main rotor radius	m, R	0.75
Main rotor chord	m, c	0.045
Helicopter mass	kg, M	5
Pitching moment of inertia	kg. m^2, I_{yy}	$3.8494*10^{-3}$
Yawing moment of inertia	kg. m^2, I_{zz}	$3.8844*10^{-3}$
Rolling moment of inertia	kg. m^2, I_{xx}	$9.3551*10^{-4}$
Main rotor blade lift curve slope	[ ], a_0	5.73

[ ]: no dimension

$$\dot{x}=Ax+Bu,\qquad y=Cx+Du \tag{9}$$

where

$$x=\begin{bmatrix}u & v & w & p & q & r & \phi_A & \theta_A & \psi_A & \beta_0 & \dot{\beta}_0 & \beta_c & \dot{\beta}_c & \beta_s & \dot{\beta}_s\end{bmatrix} \tag{10}$$

$$u=\begin{bmatrix}\theta_0 & \theta_c & \theta_s & \theta_T\end{bmatrix} \tag{11}$$

For hover and 20 km/h straight level flight conditions, the linearized state-space models respectively are

$$A_h = \begin{bmatrix}
-3.2681e-4 & -3.85833e-4 & -1.6198e-4 & -2.4915e-3 & 9.9164e-5 & 3.2964e-8 & 0 & -5.3065e-4 & 0 & 4.0464e-6 & 9.5104e-7 & -7.5876e-2 & -6.4767e-4 & -6.4766e-4 & 9.0766e-5 \\
4.3356e-4 & -4.6508e-4 & -9.8709e-5 & -1.1796e-4 & -2.7102e-3 & -2.2989e-3 & 5.3021e-4 & -7.4151e-9 & 0 & 1.4318e-6 & 6.0663e-5 & -7.2807e-4 & 4.3044e-5 & 8.5275e-2 & 7.2840e-4 \\
1.1896e-5 & 8.4786e-7 & -5.8499e-3 & -6.1579e-6 & 2.3229e-3 & 1.5773e-9 & 2.1647e-5 & 1.8162e-7 & 0 & -1.1080e-1 & -2.3233e-3 & 5.5464e-6 & -1.9896e-8 & 5.9124e-6 & 4.9234e-8 \\
-1.8716e-2 & -6.9388e-4 & 4.4618e-3 & 4.8047e-3 & 8.5840e-2 & -9.8520e-4 & 0 & 0 & 0 & 6.2037e-4 & -2.7123e-3 & 3.1655e-2 & 1.8685e-2 & -3.6868 & -3.1669e-2 \\
8.8809e-4 & -1.6653e-2 & -6.6947e-3 & -7.6382e-2 & 3.4316e-3 & 7.5606e-13 & 0 & 0 & 0 & 6.4947e-5 & -1.7206e-4 & -3.2803 & -2.8178e-2 & -2.8177e-2 & -1.6622e-2 \\
-1.9727e-3 & 2.6895e-2 & 3.0346e-1 & -4.4181e-3 & 8.3794e-3 & -9.0104e-3 & 0 & 0 & 0 & 6.5277e-5 & -1.5853e-1 & 2.3443e-3 & 2.1535e-3 & -3.7616e-1 & -3.2357e-3 \\
0 & 0 & 0 & 1 & 1.3974e-5 & -3.4226e-4 & 0 & 0 & 0 & 0 & 0 & 0 & 0 & 0 & 0 \\
0 & 0 & 0 & 0 & 9.9917e-1 & 4.0794e-2 & 0 & 0 & 0 & 0 & 0 & 0 & 0 & 0 & 0 \\
0 & 0 & 0 & 0 & -4.0794e-2 & 9.9917e-1 & 0 & 0 & 0 & 0 & 0 & 0 & 0 & 0 & 0 \\
0 & 0 & 0 & 0 & 0 & 0 & 0 & 0 & 0 & 0 & 1 & 0 & 0 & 0 & 0 \\
-7.9682e-4 & -1.8380e-4 & 1.96509 & 2.2565e-3 & 2.6790e-4 & 5.9118e-8 & 0 & 0 & 0 & -4.1527 & -1.0958 & -7.4827e-4 & -1.3943e-6 & 2.2099e-4 & -1.5989e-3 \\
0 & 0 & 0 & 0 & 0 & 0 & 0 & 0 & 0 & 0 & 0 & 0 & 1 & 0 & 0 \\
-5.3701e-3 & 1.0077e-1 & -9.7089e-3 & 2.8272 & 1.5550 & 1.0965e-12 & 0 & 0 & 0 & -4.5415e-3 & -2.4957e-4 & -7.9100 & -1.1367 & -1.1367 & -2.0241 \\
0 & 0 & 0 & 0 & 0 & 0 & 0 & 0 & 0 & 0 & 0 & 0 & 0 & 0 & 1 \\
9.7775e-2 & 5.6513e-3 & 1.2707e-2 & 1.5570 & -2.8135 & -1.4288e-3 & 0 & 0 & 0 & 8.9976e-4 & -7.1348e-3 & 1.1417 & 2.0271 & -8.4994 & -1.1418
\end{bmatrix} \quad (12)$$

$$B_h = \begin{bmatrix}
-5.5991e-7 & 3.0094e-4 & -1.6464e-4 & -2.6687e-14 \\
-1.0219e-4 & -7.8108e-5 & -3.3862e-4 & 2.9152e-4 \\
1.0795e-3 & 5.7193e-8 & -1.2773e-5 & 1.0196e-8 \\
4.5102e-3 & -3.3893e-2 & 1.4723e-2 & -6.3684e-3 \\
1.0252e-4 & 1.3093e-2 & 3.0151e-2 & 4.8872e-12 \\
2.8752e-1 & -3.8319e-3 & 2.0016e-3 & -1.2988e-1 \\
0 & 0 & 0 & 0 \\
0 & 0 & 0 & 0 \\
0 & 0 & 0 & 0 \\
0 & 0 & 0 & 0 \\
1.5478 & 2.2151e-6 & 4.6351e-3 & 3.8214e-7 \\
0 & 0 & 0 & 0 \\
1.4880e-4 & 1.56678 & 4.3727e-2 & 7.0876e-12 \\
0 & 0 & 0 & 0 \\
1.5812e-2 & -4.9154e-2 & 1.5692 & -9.2357e-3
\end{bmatrix} \quad (13)$$

$$A_{20} = \begin{bmatrix}
-7.5797e-3 & -4.7019e-4 & -1.0855e-4 & -2.5285e-3 & 1.7450e-3 & 2.5395e-4 & 0 & -5.2719e-4 & 0 & 4.7724e-5 & 4.6878e-6 & -7.5885e-2 & -6.4759e-4 & -6.4420e-4 & 1.0747e-4 \\
4.7931e-4 & -4.6890e-3 & 2.2143e-4 & -1.4830e-3 & -2.7417e-3 & -4.6357e-2 & 5.2660e-4 & -2.8562e-6 & 0 & 4.2376e-6 & 7.5574e-5 & -7.2956e-4 & 5.0862e-5 & 8.5267e-2 & 7.2926e-4 \\
1.2964e-4 & 1.9271e-5 & -6.9605e-3 & -3.7298e-4 & 4.6703e-2 & 4.9579e-8 & 2.4889e-5 & 6.0430e-5 & 0 & -1.1080e-1 & -2.3233e-3 & 1.6990e-4 & 3.1813e-7 & 1.3751e-5 & 2.7397e-7 \\
-2.1050e-2 & 1.2854e-1 & -1.3390e-2 & -1.2199e-1 & 8.3814e-2 & -1.3003e-2 & 0 & 0 & 0 & 1.5159e-3 & -1.5154e-3 & 3.1888e-2 & 2.1985e-2 & -3.68183 & -3.1656e-2 \\
-2.1982e-1 & -2.0065e-2 & -1.0724e-2 & -7.4387e-2 & -1.1159e-1 & -1.3197e-9 & 0 & 0 & 0 & 7.2683e-3 & -8.5389e-4 & -3.2759 & -2.8169e-2 & -2.7973e-2 & -1.9663e-2 \\
-3.5038e-4 & 1.6783e-1 & 3.0936e-1 & -8.7136e-2 & 1.1132e-2 & -3.2839e-2 & 0 & 0 & 0 & -4.5117e-4 & -1.8697e-1 & -2.9876e-3 & 2.2373e-3 & -3.7003e-1 & -5.5503e-3 \\
0 & 0 & 0 & 1 & 5.4178e-3 & -1.1463e-1 & 0 & 0 & 0 & 0 & 0 & 0 & 0 & 0 & 0 \\
0 & 0 & 0 & 0 & 9.9888e-1 & 4.7212e-2 & 0 & 0 & 0 & 0 & 0 & 0 & 0 & 0 & 0 \\
0 & 0 & 0 & 0 & -4.7521e-2 & 1.0054 & 0 & 0 & 0 & 0 & 0 & 0 & 0 & 0 & 0 \\
0 & 0 & 0 & 0 & 0 & 0 & 0 & 0 & 0 & 0 & 1 & 0 & 0 & 0 & 0 \\
8.7542e-4 & -6.5356e-3 & 1.9651 & 4.3877e-2 & 5.5115e-5 & 1.8582e-6 & 0 & 0 & 0 & -4.1527 & -1.0958 & -1.2636e-2 & -1.6154e-4 & 6.1717e-4 & -3.1791e-2 \\
0 & 0 & 0 & 0 & 0 & 0 & 0 & 0 & 0 & 0 & 0 & 0 & 1 & 0 & 0 \\
-3.2399e-1 & 1.0509e-1 & -1.4876e-2 & 2.8332 & 1.3878 & -1.9132e-9 & 0 & 0 & 0 & -8.1573e-2 & -1.5825e-3 & -7.9020 & -1.1367 & -1.1378 & -2.0285 \\
0 & 0 & 0 & 0 & 0 & 0 & 0 & 0 & 0 & 0 & 0 & 0 & 0 & 0 & 1 \\
1.0318e-1 & 1.9124e-1 & 1.0450e-1 & 1.3726 & -2.8193 & -1.8852e-2 & 0 & 0 & 0 & 2.6967e-3 & -6.5807e-2 & 1.1406 & 2.0319 & -8.4904 & -1.1417
\end{bmatrix} \quad (14)$$

$$B_{20} = \begin{bmatrix}
-1.7842e-5 & 2.9734e-4 & -1.8659e-4 & 3.5322e-12 \\
3.4149e-5 & -8.8481e-5 & -3.3200e-4 & 2.9148e-4 \\
1.0537e-3 & -1.3976e-6 & -2.5397e-4 & 2.4280e-8 \\
-1.4278e-3 & -3.8296e-2 & 1.4442e-2 & -6.3683e-3 \\
3.0913e-3 & 1.2927e-2 & 3.4133e-2 & -6.4630e-10 \\
3.2484e-1 & -4.1033e-3 & 1.6472e-2 & -1.2986e-1 \\
0 & 0 & 0 & 0 \\
0 & 0 & 0 & 0 \\
0 & 0 & 0 & 0 \\
0 & 0 & 0 & 0 \\
1.5507 & 4.9812e-4 & 9.2091e-2 & 9.1005e-7 \\
0 & 0 & 0 & 0 \\
5.4797e-3 & 1.5680 & 4.9500e-2 & -9.3698e-10 \\
0 & 0 & 0 & 0 \\
1.8215e-1 & -5.5504e-2 & 1.5731 & -9.2324e-003
\end{bmatrix} \quad (15)$$

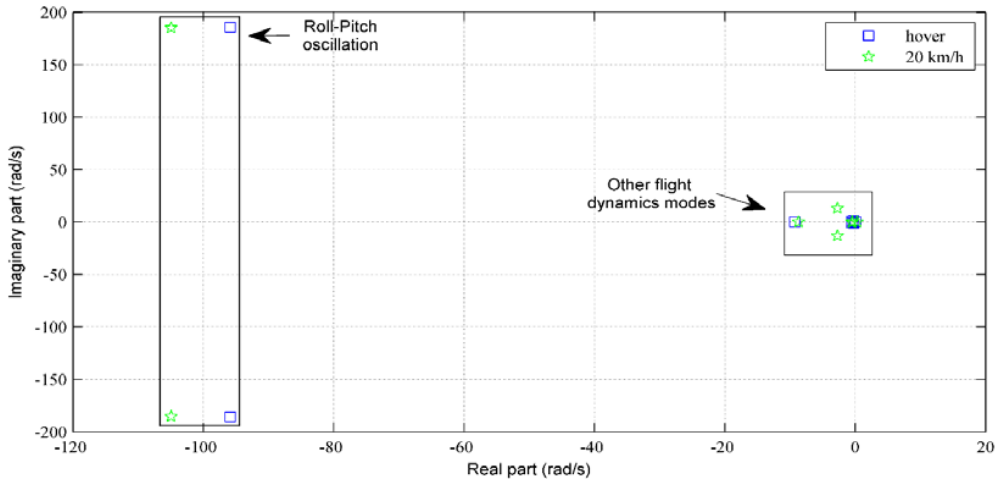

(a)

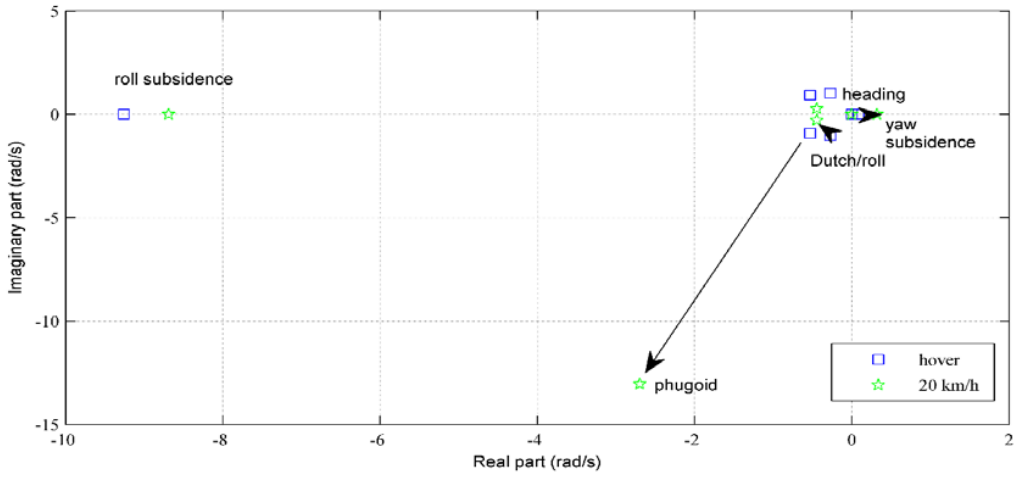

(b)

Fig. 2 Flight Dynamics Modes of ZANKA-Heli-I (a) All the modes (b) Zoomed ones

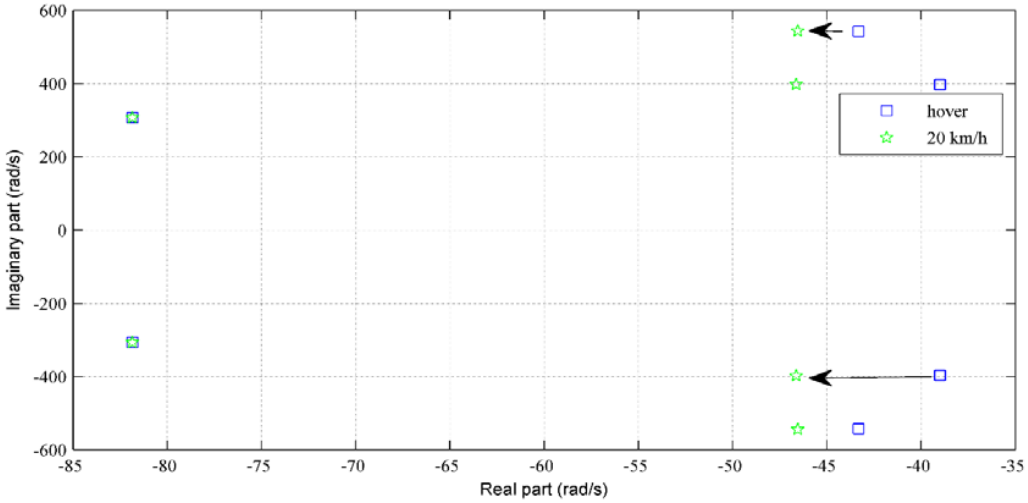

Fig. 3 Flapping Modes of ZANKA-Heli-I

III. Autopilot System

For our both theoretical and practical (with real-time flight tests) studies traditional PID based hierarchical autopilot system is chosen [6], [7]. It uses three layers PID controller to accomplish waypoint navigation (Fig. 4). In Fig. 5 more detailed version of PID-based hierarchical autopilot system is given. In Fig. 6 an Ardupilot equipped UAV is given.

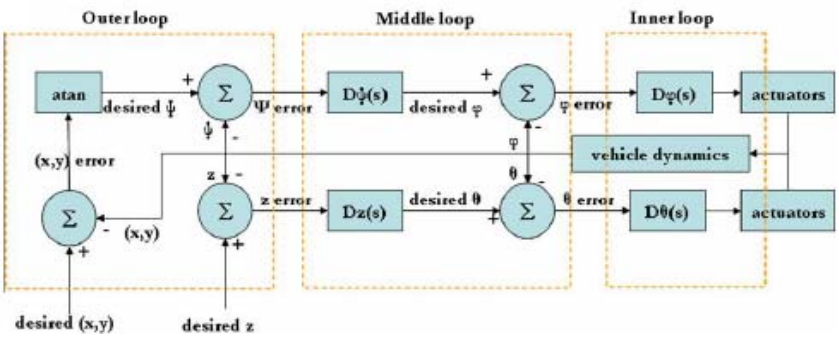

Fig. 4 Hierarchical Autopilot System [6]

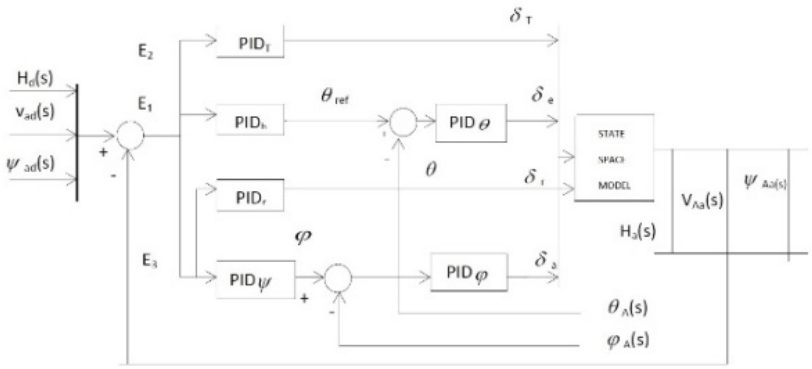

Fig. 5 General PID Based Autopilot Structure

Fig. 6 Autopilot Equipment of ZANKA UAV

IV. Problem Formulation

In most overall usage PID based hierarchical autopilot system permits height, yaw angle, and velocity tracking. This autopilot system has 6 P-I-D controllers in 3 layers (outer, middle, inner). These PIDs have upper and lower bounds and satisfy trajectory tracking. If any interested autopilot user demands to use all of them, it is required to adjust 18 parameters (i.e. 6 P parameters, 6 I parameters and 6 D parameters). A cost function consisting of settling time, rise time and overshoot is respectable choice for high-performance trajectory tracking.

$$\boldsymbol{J} = T_{rt} + T_{st} + OS \tag{16}$$

The control system optimization problem can be defined as:

$min\{\boldsymbol{J}\}$ where

$$\boldsymbol{J} = f\left(K_{P_1}, K_{I_1}, K_{D_1}, K_{P_2}, K_{I_2}, K_{D_2}, \ldots\ldots\ldots\ldots, K_{P_6}, K_{I_6}, K_{D_6}\right) \tag{17}$$

and it is function of 18 terms (18 autopilot system design parameters).

V. Optimization Method

Since there is complex dependency between $\boldsymbol{J}$ (see Eq. (9)) and the constraints on the optimization variables (18 P-I-D gains), computation of cost function derivatives with respect to these parameters is not analytically possible. This advocates the claim of certain stochastic optimization techniques. In order to solve this complex problem for this paper, we choose a stochastic optimization method called as SPSA, which was successfully used in similar complex constrained optimization problems previously [8]-[10]. SPSA has many advantages w.r.t. the other current method in the literature. First of all, SPSA is low-cost since it uses only two evaluations of the objective to guess the gradient [11], [12]. Furthermore, it is also successful in solving constrained optimization problems.

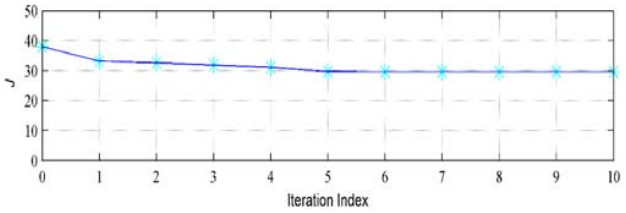

Fig. 7 Cost Minimization

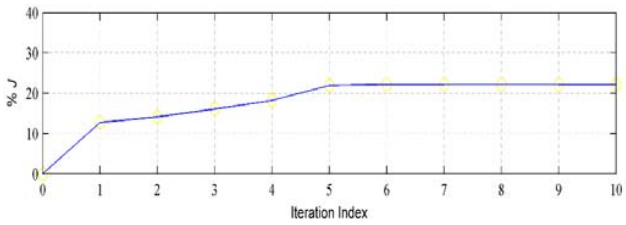

Fig. 8 Relative Cost Minimization

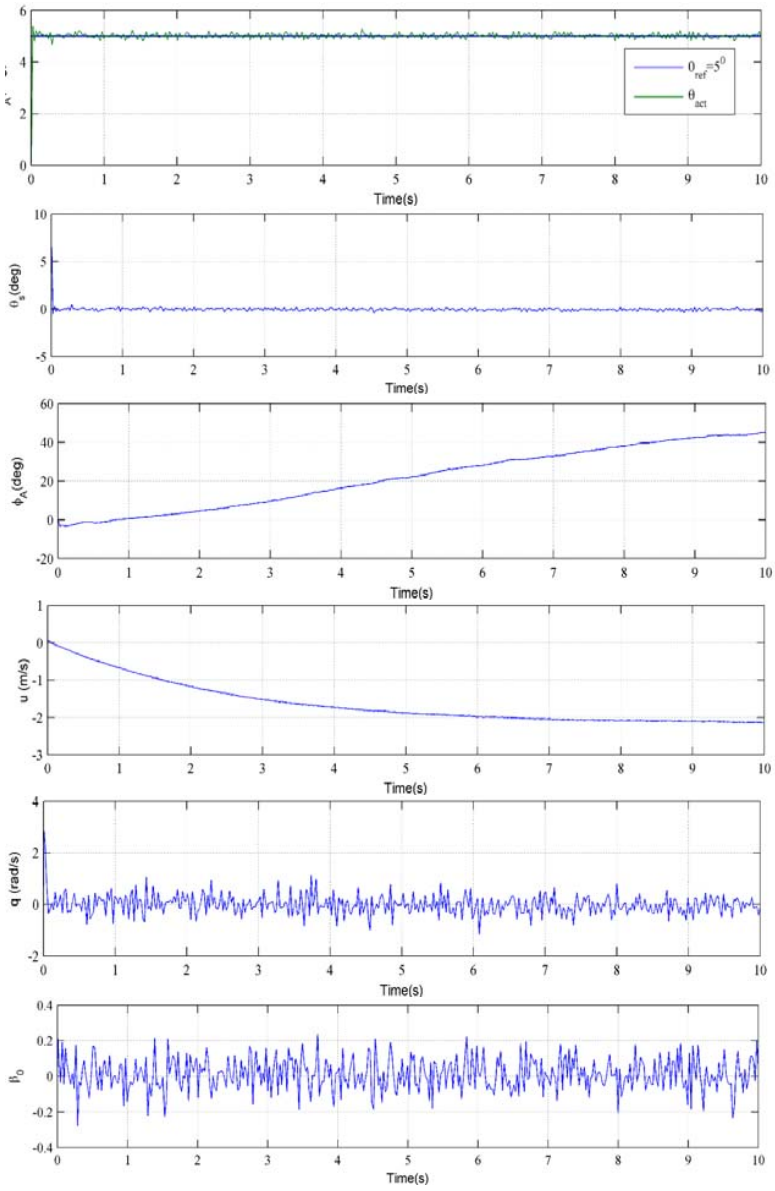

Fig. 9 Closed Loop Responses after Redesign

VI. Simulation Results

After optimizing control system in order to minimize cost optimum P, I, D values are determined. In Figs. 7 and 8 cost minimization and relative energy save are given, respectively. Around %23 of the cost is saved after optimizing autopilot system.

Success of regulated autopilot system when there is noise on the system (i.e. Gaussian white noise with spectral density of 10^-4) is also investigated. In Fig. 9 the closed loop system responses when there is white noise on the system are given.

From this figure, it can be seen that when there is also noise on the system, the autopilot system is able to track reference trajectory effectively. Furthermore, other states do not experience fast and large oscillations during this pitch trajectory tracking. Final, while there is constraint on control surface (+-10 degrees for elevator), it is also feasible for desired trajectory tracking

VII. Conclusions

In this paper, autonomous performance of a small manufactured unmanned helicopter is tried to be maximized. For this reason, a small unmanned helicopter is produced in Erciyes University, Faculty of Aeronautics and Astronautics. It is named as ZANKA-Heli-I. In order to maximize performance, autopilot parameters are determined via minimizing a cost function consisting of flight performance parameters such as settling time, overshoot during trajectory tracking. For this reason, a stochastic optimization method named as simultaneous perturbation stochastic approximation is applied. Using this approach considerable autonomous performance rise (around %23) is obtained.

Acknowledgment

This work was supported by Research Fund of the Erciyes University, Project Number: FBA-2015-5954.

References

[1] R. Austin, *Unmanned aircraft systems*. Wiley, 2010.
[2] S. Kim, A. Budiyono, J. H. Lee, D. H. Kim, K. J. Yoon, Control system design and testing for a small-scale autonomous helicopter, Aircraft Engineering and Aerospace Technology, 82(6), 353-359, 2010.
[3] H. Reza Dharmayanda, A. Budiyono and T. Kang, State-space identification and implementation of H_∞ control design for small-scale helicopter, Aircraft Engineering and Aerospace Technology, 82(6), 340-352, 2010.
[4] I. B. Tijani, R. Akmeliawati and A. Legowa, H_∞ robust controller for autonomous helicopter hovering control, Aircraft Engineering and Aerospace Technology, 83(6), 363-374, 2011.
[5] E. Joelianto, E. M. Sumarjano, A. Budiyono, D. R. Penggalih, Aircraft Engineering and Aerospace Technology, 83(6), 363-374, 2011.
[6] Chao, H., Cao, Y., and Chen, Y. Q. 2007. Autopilots for Small Fixed-Wing Unmanned Aerial Vehicles: A Survey. Paper presented at IEEE International Conference on Mechatronics and Automation, Harbin, China.
[7] Jang, J. S., Liccardo, D. 2006. Automation of small UAVs using a low cost mems sensor and embedded computing platform.
[8] C. Sultan Proportional damping approximation using the energy gain and simultaneous perturbation stochastic approximation. Mechanical Systems and Signal Processing. 24, 2210-2224, 2010.
[9] T. Oktay. Constrained control of complex helicopter models. PhD Dissertation, Virginia Tech, 2012.
[10] T. Oktay and C. Sultan. Simultaneous helicopter and control-system design," *Journal of Aircraft*, Vol. 50, No. 3, pp. 32-47, 2013.
[11] P. Sadegh and J. C. Spall, Optimal random perturbations for multivariable stochastic approximation using a simultaneous perturbation gradient approximation", IEEE Transactions on Automatic Control, 43(10), pp. 1480-1484, 1998.
[12] Y. He and M. C. Fu, Convergence of simultaneous perturbation stochastic approximation for non-differentiable optimization, IEEE Transactions on Aerospace and Electronic Systems, 48(8), 1459-1463, 2003.